

Tuning the phase diagram of a Rosenzweig-Porter model with fractal disorder

Madhumita Sarkar*

Jožef Stefan Institute, SI-1000 Ljubljana, Slovenia

Roopayan Ghosh

Department of Physics and Astronomy, University College London, Gower Street, London WC1E 6BT, United Kingdom

Ivan M. Khaymovich

Nordita, Stockholm University and KTH Royal Institute of Technology Hannes Alfvéns väg 12, SE-106 91 Stockholm, Sweden
and Institute for Physics of Microstructures, Russian Academy of Sciences, 603950 Nizhny Novgorod, GSP-105, Russia



(Received 6 June 2023; accepted 10 August 2023; published 29 August 2023)

The Rosenzweig-Porter (RP) model has garnered much attention in the last decade, as it is a simple analytically tractable model showing both ergodic-nonergodic extended and Anderson localization transitions. Thus, it is a good toy model to understand the Hilbert-space structure of many-body localization phenomenon. In our Letter, we present analytical evidence, supported by exact numerics, that demonstrates the controllable tuning of the phase diagram in the RP model by employing on-site potentials with a nontrivial fractal dimension instead of the conventional random disorder. We demonstrate that such disorder extends the fractal phase and creates an unusual dependence of fractal dimensions of the eigenfunctions. Furthermore, we study the fate of level statistics in such a system to understand how these changes are reflected in the eigenvalue statistics.

DOI: [10.1103/PhysRevB.108.L060203](https://doi.org/10.1103/PhysRevB.108.L060203)

Introduction. The disorder-induced breakdown [1–4] of quantum ergodicity [5,6], referred to as many-body localization (MBL), is a generic phenomenon in many-body (MB) systems. Being a localized phase in real space, MBL provides only ergodicity breaking in its Hilbert counterpart [7–9]. This fact as well as the discovery of nonergodic extended phases in MB systems [10–21] as an intermediate regime between ergodic and localized phases [1,22–27] necessitated the search for analytically tractable toy models to understand this phenomenon. One direction of this search is based on the random-matrix ensembles that mimic the Hilbert-space properties of such MB systems in a controlled fashion. The Rosenzweig-Porter (RP) random-matrix model [28] provides such an example which has been studied extensively in recent years as it allows almost a complete analytical understanding of the phase diagram [29–34], and a perturbative (exact in the thermodynamic limit) description [35] of the eigenspectrum for a wide range of parameter values.

The RP model is given by the Gaussian random-matrix ensemble of size L , where each element is random number obtained from a normal distribution, and the off-diagonal

elements are rescaled by a factor of $L^{-\gamma/2}$,

$$H_{mn} = h_n \delta_{mn} + M_{mn} L^{-\gamma/2}, \quad (1)$$

where $\overline{h_n} = \overline{M_{mn}} = 0$, $\overline{h_n^2} = \overline{M_{mn}^2} = 1$. It has been shown that [29,30], with increasing γ from 0 to large values, this model first exhibits ergodicity, and then undergoes a transition to a nonergodic extended (fractal) phase at $\gamma = 1$. In the fractal phase the eigenfunction support sets contain an extensive number, but measure zero of all the lattice sites, scaling as L^D , where $D = 2 - \gamma$ denotes the second fractal dimension of the eigenfunction (the precise definition of D is provided in the next section). As is immediately apparent, $D = 1$ corresponds to the ergodic phase. Furthermore, at $\gamma = 2$, D goes linearly to 0, marking the onset of the Anderson localized phase. Although this version of the model lacks the genuine multifractality in its eigenfunctions, recent developments [32,36–40] show that some modified versions of this model may exhibit multifractality. Further studies [41] demonstrated the instability of the nonergodic extended phase in a non-Hermitian version of the model. Unlike the latter case, in this Letter we show how to extend the range and stability of the fractal phase of the RP model by employing a “fractal” on-site disorder. We also include the possibility of obtaining a nonlinear dependence of the fractal dimension on the parameter, γ .

Summary of results. In our study, we selectively employ a random normal distribution solely for the off-diagonal elements of H , while the diagonal elements (H_{mm}) are sourced from a “fractal” disorder distribution with a Hausdorff dimension of d . This implies that there are typically $L^{1-d \times b}$ random diagonal elements, present in an energy window of

*sarkar.madhumita770@gmail.com

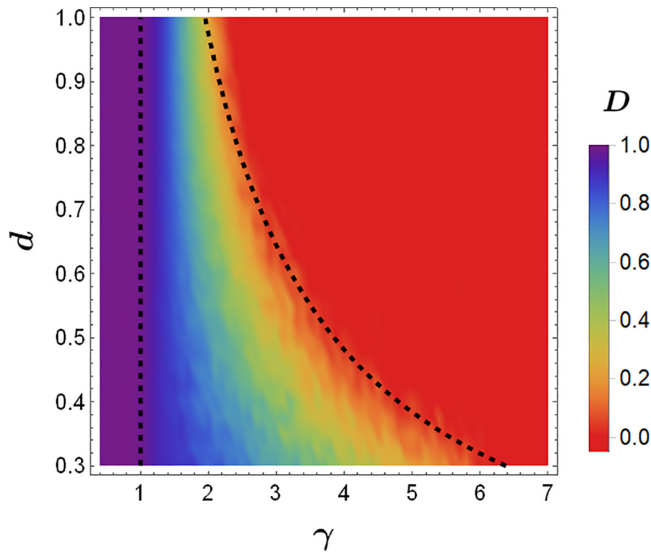


FIG. 1. Fractal dimension D vs γ and the Hausdorff dimension d , showing good agreement with the analytical predictions of ergodic, $\gamma_{ET} \simeq 1$, and Anderson, $\gamma_{AT} \simeq 2/d$, transitions (black dotted lines) [Eq. (10)]. Numerically, in Figs. 1–4, D has been obtained by fitting the inverse participation ratio (IPR) [Eq. (2)] of the eigenvectors for system sizes $L = 2^p$, $7 \leq p \leq 12$.

width L^{-b} , if the total bandwidth is taken to be $O(1)$. One of the well-known examples of such a distribution is the Cantor set with a Hausdorff dimension [42] $d = \ln 2 / \ln 3$.

The main result of our work is shown in Fig. 1, where we represent the extended phase diagram of the RP model in terms of the second fractal dimension obtained from numerical fits of the generalized IPR,

$$\text{IPR}_j^{(q)} = \sum_i^L |i|\chi_j|^{2q}, \quad (2)$$

for $q = 2$, where $|i\rangle$ denotes computational basis states and $|\chi_j\rangle$ denotes an eigenvector with index j . Then $\text{IPR}^{(2)} \sim L^{-D_2}$, where D_2 is the second fractal dimension, and one obtains D_2 from averages over numerical fits from a band of eigenvectors. D_2 can then be used to distinguish between the ergodic ($=1$), nonergodic extended, i.e., fractal ($0 < D_2 < 1$), and Anderson localized phase ($=0$). We refer to D_2 as D since the higher moments show the same value, i.e., $D_q = D_2$, $q > 1/2$, thus indicating that the eigenfunctions are fractal and not multifractal. In Fig. 1, we plot the γ and d dependence of D . We note the following from the plot:

(1) $d = 1$ represents the case for the generic RP model and the ergodic-fractal transition occurs at $\gamma = \gamma_{ET} = 1$ and the Anderson transition occurs at $\gamma = \gamma_{AT} = 2$ replicating the known results [29].

(2) As the Hausdorff dimension of the diagonal elements decreases, γ_{ET} is intact, but γ_{AT} monotonically increases, extending the fractal phase in γ .

(3) Both the transitions can be very well approximated by perturbative analytical expressions, which become exact in the thermodynamic limit, denoted by black dashed lines in the plot.

It is also worth mentioning that, for $d > 1$, the phase diagram shows similar behavior as for $d = 1$. This is because beyond the physical dimension of the diagonal disorder [one dimension (1D) in our Hermitian case], any increase in fractal dimension cannot have an effect [43].

In what follows, we first analytically calculate the fractal dimension for eigenfunctions of the fractal RP model with changing γ and d . Then we compare the obtained expressions with exact numerics performed for (i) the commonly studied Cantor set fractal distribution, and then (ii) for a distribution with arbitrary Hausdorff dimensions d , suggested in Ref. [42]. For completeness, we also discuss the level spacing statistics in such a model, and in the Supplemental Material [44] discuss the time-dependent survival probability of a wave packet, initially localized at a single site.

Analytical phase-diagram calculations. As mentioned before, we consider the h_n 's to be distributed in a fractal (and later multifractal) manner [45]. This implies that the h_n 's are distributed such that, the number (N) of h_n 's in a given energy interval $|E - h_n| \in [L^{-b-db}, L^{-b}]$, parametrized by b ($db \lesssim 1/\ln L$), vary as

$$N\{|E - h_n| \in [L^{-b-db}, L^{-b}]\} \equiv L^{1-f(b)} db, \quad (3)$$

with a certain $f(b) \leq 1$, characterizing the above fractal (note db here denotes small changes in b and d is not to be confused with Hausdorff dimension d). We also assume that the overall bandwidth of the h_n is $\sim O(1) = L^0$. Thus, $f(0) = 0$. For any generic fractal with the Hausdorff dimension d we will have

$$f(b) = d \cdot b, \quad (4)$$

For the special case of the Cantor set, $d = \ln 2 / \ln 3$. Note that, in general, $f(b)$ can depend on E , but for the case of the Cantor set E dependence arises only in $1/\ln L$ corrections to $f(b)$ beyond the saddle-point expression (3). In contrast, in the case of uniform disorder distribution, the number of h_n 's is proportional to the width of the energy interval, i.e., $f(b) = b$. Thus the usual Hermitian case [29] corresponds to $d = 1$, while the non-Hermitian complex one [41] gives $d = 2$.

The above saddle-point consideration in Eq. (3) is valid as soon as the number $L^{1-f(b)} \gg 1$ is large. As we will see below, this corresponds to delocalized phases, where all the energy intervals are much larger than the typical level spacing δ_{typ} , i.e., the energy interval where one typically finds a single energy level. Indeed, the typical level spacing of the disorder δ_{typ} is given by

$$\begin{aligned} N = L^{1-f(b_{\text{typ}})} = 1 &\Leftrightarrow f(b_{\text{typ}}) = 1 \\ \Leftrightarrow b_{\text{typ}} = 1/d &\Leftrightarrow \delta_{\text{typ}} = L^{-b_{\text{typ}}} = L^{-1/d}. \end{aligned} \quad (5)$$

In this work, we focus only on real entries and thus work in the scenario $0 < d < 1$. The generalization to the non-Hermitian matrices to cover $0 \leq d \leq 2$ is straightforward. In what follows, we provide a short description of computation of the fractal dimension of a typical eigenstate of this model and thus compute γ_{AT} and γ_{ET} .

Using the standard cavity Green's function method, we can find a self-consistency equation for the level broadening (the imaginary part of the self energy) Γ_m as (see Supplemental

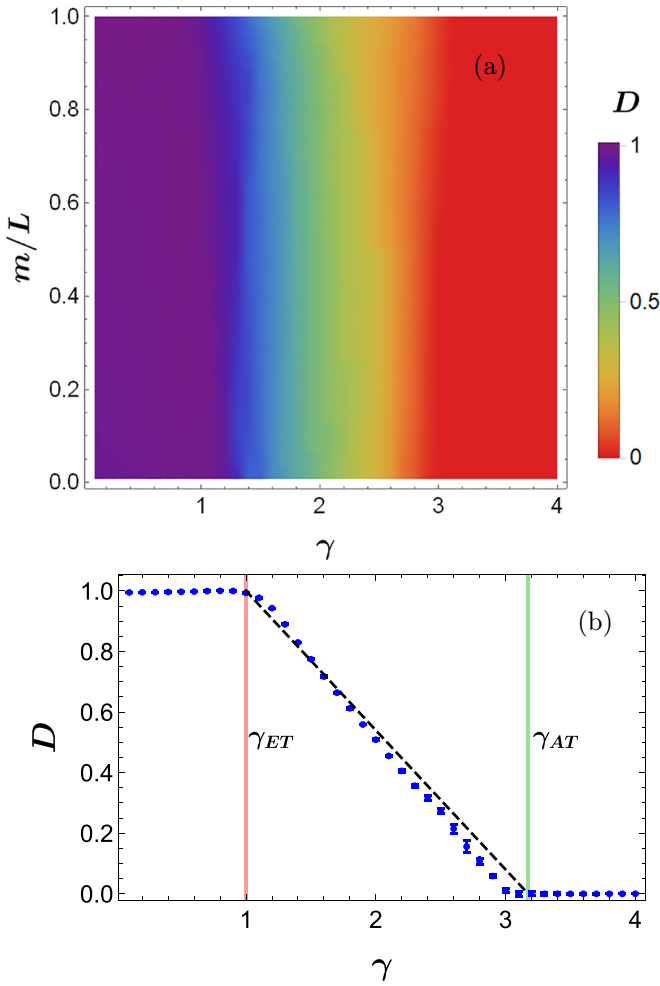


FIG. 2. (a) Energy-resolved fractal dimension D vs γ and eigenstate index m (sorted in increasing order of IPR) for Cantor set disorder. (b) Spectral-averaged fractal dimension (blue dots) vs γ , averaged over all eigenstates. The black dashed line indicates the analytical prediction [Eq. (10)] for D at $1 < \gamma < \gamma_{AT}$, with $d = \frac{\ln 2}{\ln 3} \sim 0.63$. The red (green) vertical line indicates the theoretical predictions of the $\gamma_{ET} = 1$ [γ_{AT} , Eq. (11)].

Material [44] and Refs. [30,32,33]),

$$\bar{\Gamma} = \frac{1}{L} \sum_n \Gamma_n = \sum_n \frac{L^{-\gamma} (\bar{\Gamma} - \eta)}{(E - h_n)^2 + (\bar{\Gamma} - \eta)^2}, \quad (6)$$

where E is the eigenenergy of the corresponding eigenvector and η is a small regularizer. The parametrization $\bar{\Gamma} = L^{-a}$ in the limit $\eta \rightarrow 0$ gives the following result from Eq. (6) within the saddle-point approximation (see Supplemental Material [44])

$$1 \sim L^{1-\gamma+2a-f(a)} \Leftrightarrow \gamma = 1 + 2a - f(a). \quad (7)$$

This determines $\Gamma \sim L^{-a}$ via the parameter γ and works for $\Gamma \gg \delta_{\text{typ}}$.

The corresponding fractal dimension $D_q \equiv D$ is determined via the number of levels located in the interval $\Gamma \sim L^{-a}$. This number is related to the fractal dimension as L^D . From Eq. (3), we know that this is given by $L^{1-f(a)}$. Thus,

$$D = 1 - f(a). \quad (8)$$

This definition of D is the fractality in the “space” of h_n , but for the RP-like fractal phases it is equal to the spatial fractal dimension due to the Lorentzian structure of the eigenstates [32,33,41,46,47]:

$$\langle |\psi_E(n)|^2 \rangle_{H_{m \neq n}} \sim \frac{1}{(E - h_n)^2 + \Gamma^2}. \quad (9)$$

As by fixing either E or h_n , one has the Lorentzian, the fractality over the energy E and over the “space” h_n is equivalent to each other. In space n , the above Lorentzian forms a fractal miniband [42] of width Γ , with the underlying fractal structure h_n , living in that miniband, $|h_n - E| \lesssim \Gamma$.

In the fractal case of Eq. (4), we obtain for $\gamma > 1$ using Eqs. (7) and (8),

$$D = \max \left(1 - d \frac{\gamma - 1}{2 - d}, 0 \right), \quad \Gamma \sim L^{-\frac{\gamma-1}{2-d}}. \quad (10)$$

The Anderson transition point corresponds to $\Gamma \simeq \delta_{\text{typ}}$, i.e., $D = 0$, since in the localized phase the number of energy levels within the Lorentzian bandwidth becomes an intensive quantity. Hence, $a = b_{\text{typ}} = 1/d$ and

$$\gamma_{AT} = 2/d. \quad (11)$$

The ergodic transition occurs at $\Gamma \sim O(1)$, $\gamma_{ET} = 1$. Note that both γ_{ET} and γ_{AT} are continuous transitions, unlike the fat-tailed distributed RP models [36–38].

Cantor set diagonal elements. The first example we consider is when the diagonal elements are represented by the Cantor set \mathcal{C} . The Cantor set is a set of points lying in a line segment normalized to the interval $[0,1]$, obtained by removing the middle third of the continuous line segments in a recursive manner. The set generated by the first few iterations of this are

$$\begin{aligned} \mathcal{C}_0 &= [0, 1], \\ \mathcal{C}_1 &= \left[0, \frac{1}{3}\right] \cup \left[\frac{2}{3}, 1\right], \\ \mathcal{C}_2 &= \left[0, \frac{1}{9}\right] \cup \left[\frac{2}{9}, \frac{1}{3}\right] \cup \left[\frac{2}{3}, \frac{7}{9}\right] \cup \left[\frac{8}{9}, 1\right], \\ &\dots \end{aligned} \quad (12)$$

We generate the diagonal elements by choosing the boundary value of each subset at the $n = \log_2 L$ iteration. The self-similar nature of the Cantor set is evident from the construction and the Hausdorff dimension is calculated to be $d = \frac{\ln 2}{\ln 3}$ [48]. In Fig. 2(a) we plot the second fractal dimension $D_2 = D$ calculated from the numerical fitting in system size 2^p , $p = 7 \dots 12$, for all the eigenvectors arranged in increasing order of IPR. In Fig. 2(b) we plot the same quantity, but averaged over 60 midspectrum states. From Fig. 2(a) it can be clearly seen that there is no mobility edge in the spectrum, and all the eigenstates show similar fractal dimensions D , hence one can average over them, which is plotted in Fig. 2(b). The point where the system ceases to be ergodic is clearly visible at $\gamma = \gamma_{ET} = 1$. Furthermore, the variation of the fractal dimension of the eigenfunctions D matches sufficiently well with the analytically obtained black dashed line [Eq. (10)] in the $\gamma_{ET} < \gamma < \gamma_{AT}$ regime, thus accurately predicting the

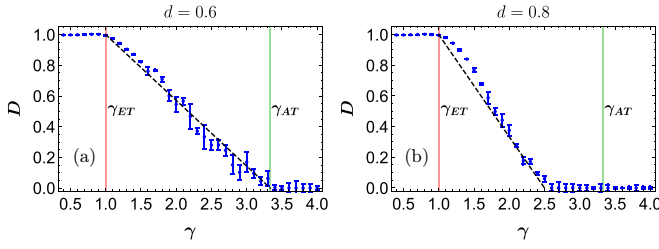


FIG. 3. Fractal dimension D vs γ , averaged over all eigenstates, for generic fractal diagonal disorder with Hausdorff dimension (a) $d = 0.6$ and (b) $d = 0.8$. The lines are the same as in Fig. 2.

γ_{AT} point as well. Finite-size effects, given by $1/\ln L$ terms in $D(L)$, are maximal close to γ_{AT} and of the magnitude ~ 0.1 .

Generic fractal diagonal elements. Next, we consider the case of generic fractal diagonal elements. The generation of diagonal elements distributed in a generic fractal dimension was introduced recently in Ref. [42], so this section also serves as a demonstration of applicability of the technique. Below, we give a short summary of the method.

A random fractal spectrum of Hausdorff dimension d can be generated using independent and identically distributed non-negative level spacings of ordered $h_n \leq h_{n+1}$,

$$s_n \equiv h_{n+1} - h_n \Leftrightarrow h_n = h_0 + \sum_{k=0}^{n-1} s_k, \quad (13)$$

which are distributed as a Pareto distribution [49]

$$P(s) = \frac{d\delta_{\text{typ}}^d}{s^{d+1}} \theta(s - \delta_{\text{typ}}), \quad (14)$$

where $\delta_{\text{typ}} \sim L^{-1/d}$ is the typical level spacing of the model and we omit the subscript n for brevity. Indeed, one can count

$$D(\gamma) = \begin{cases} 1, & \gamma < 1, \\ 2 - \gamma, & 1 < \gamma < 3 - \nu_0, \\ \gamma + 6\nu_0 - 8 - 4\sqrt{(\nu_0 - 1)(\gamma + 2\nu_0 - 4)}, & 3 - \nu_0 < \gamma < 2\nu_0, \\ 0 & \gamma > 2\nu_0, \end{cases} \quad (17)$$

where the Anderson transition happens at $D = 0$, i.e., at $b = \nu_0$ and $\gamma = 2\nu_0$. The above formula works for $1 < \nu_0 < 2$. Note that unlike the fractal case, here there are four regimes: (i) the ergodic phase, $\Gamma \gg O(1)$; (ii) the usual fractal case, $\delta \ll \Gamma \ll O(1)$; (iii) the new fractal case, $\delta_{\text{typ}} \ll \Gamma \ll \delta$; and (iv) the localized phase, $\Gamma \ll \delta_{\text{typ}}$. Here, the unusual fractal phase (iii) appears only when the mean level spacing δ converges and differs from the typical one, $\delta_{\text{typ}} \ll \delta \ll O(1)$.

The results are plotted in Fig. 4 where the predicted fractal dimensions from our saddle-point approximation match well with exact numerical results. We clearly see a curvature in D vs γ , a feature absent in the fractal case, which increases with increasing ν_0 . However, it seems that finite-size effects are stronger in this case than for fractal disorder, due to the logarithmic dependence of the prefactors in Eq. (16) (see similar effects in Refs. [36,37,39]). Indeed, here finite-size effects to $D(L)$ are given by $\ln \ln L / \ln L$, that for available system sizes give 2.5 times larger deviations.

that for the usual Cantor set with $d = \ln 2 / \ln 3$, and at the n th step one keeps $L \cdot P(s) \sim 2^n$ levels with the spacings $s \sim 3^{-n}$, leading to the above expression. Due to the formal divergence of the mean level spacing for all $d < 1$ at large s , for any finite L one should put an upper cutoff $s_{\text{max}} \sim O(1)$, given by the entire bandwidth,

$$\delta = \langle s \rangle \sim \int_{\delta_{\text{typ}}}^{s_{\text{max}}} s P(s) ds \sim \delta_{\text{typ}}^d \sim L^{-1}, \quad (15)$$

and consider a typical realization where there is only one $s_n \simeq s_{\text{max}} \simeq O(1)$, determining the bandwidth. In Figs. 3(a) and 3(b) we demonstrate how our theoretical predictions of D match with numerical results for $d = 0.6$ and $d = 0.8$. We see that even for generic dimensions our analytical predictions match very well with numerics.

Multifractal disorder. As a final example, we consider the more general case of multifractal disorder. Unlike the fractal case, where the scaling behavior of all the moments of the distribution are the same, in a multifractal they are a nontrivial function of the moment order. Thus, one needs to define the probability distribution of level spacings in an energy window appropriately scaling with system size. In this case the probability distribution of level spacings is given by [44]

$$P(s \sim L^{-\nu}) ds = \sqrt{\frac{|g'(\nu_0)| \ln L}{2\pi}} L^{g(\nu)-1} d\nu, \quad (16)$$

where $g(\nu)$ is a nonlinear function of ν . As an example we consider a particular case of the log-normal distribution where $g(\nu) = 1 - \frac{(\nu - \nu_0)^2}{4(\nu_0 - 1)}$.

Then we can compute the fractal dimension D (see Supplemental Material [44]) as

Level statistics. Until now, our focus has been exclusively on the properties of the eigenfunctions. To provide a complete analysis, we shall now study the behavior of a signature of the phase transition in the energy levels, the consecutive level spacing ratio r defined by

$$r = \frac{\min(\delta_n, \delta_{n+1})}{\max(\delta_n, \delta_{n+1})}, \quad (18)$$

where $\delta_n = E_n - E_{n+1}$, and E_n is the n th eigenvalue when they are sorted in increasing order. In the ergodic phase, it is well known that for the Gaussian orthogonal ensemble (GOE) $\langle r \rangle \sim 0.53$ [50,51], where $p(r) = \frac{27}{4} \frac{r+r^2}{(1+r+r^2)^{5/2}}$. Deep in the localized phase we analytically derive that

$$p(r) = \frac{d}{r^{1-d}}, \quad \text{which gives } \langle r \rangle = \frac{d}{d+1}. \quad (19)$$

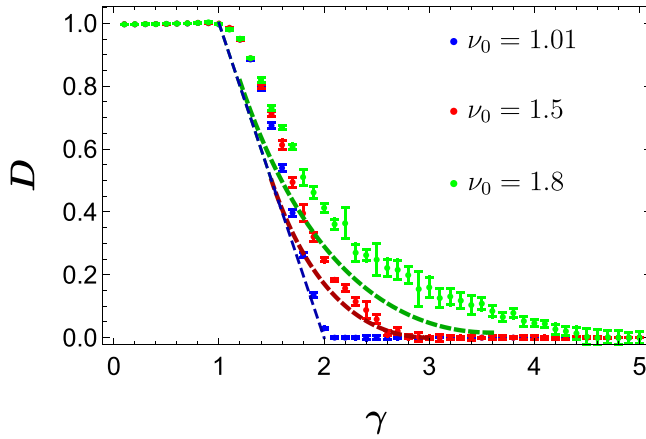


FIG. 4. $D(\gamma)$ vs γ for the log-normal disorder [Eq. (16)] with $\nu_0 = 1.01$ (blue), $\nu_0 = 1.5$ (red), $\nu_0 = 1.8$ (green). The dotted lines are the analytical predictions of $D(\gamma)$ from Eq. (17).

In Fig. 5 we plot the variation of $\langle r \rangle$ with γ for different d . As expected from our analysis for $\gamma < \gamma_{ET} = 1$, it admits a value close to 0.53, while at large $\gamma > \gamma_{AT} = 2/d$, it settles at $\sim \frac{d}{d+1}$ [Eq. (19)]. It admits intermediate values in the fractal regime, and the span in γ where such values are observed increases with smaller d , consistent with our previous results. As the smaller d values correspond to the fatter distribution tail [Eq. (14)], the finite-size effects are stronger.

According to Eq. (9), γ dependence of $\langle r \rangle$ goes to a kink at $\gamma = \gamma_{AT}$ in the thermodynamic limit. It is interesting to note here that the fractal value $r = d/(d+1)$ covers the range from 0 (well below the Poisson value at $d = 0$) to 0.5 (rather close to the GOE one at $d \rightarrow 1$). This means that if in some other models the fractal spectrum emerges, it can be mistakenly associated with the Poisson, Wigner-Dyson, or any other statistics, based solely on r statistics. Another interesting aspect is another “kink,” observed in the plots for $d \gtrsim 0.9$. While the first kink is due to a breakdown of level repulsion, the second kink occurs due to the fat tail of $P(r)$ in the localized phase for $d \sim 1$. When the weight of large r values for nonhybridized eigenstates deep inside the localized phase become significantly larger than what it was in the ergodic or fractal phase, it shows up as a slight increase in $\langle r \rangle$. (Also see Supplemental Material [44].)

Discussion. In this Letter, we have demonstrated that making the distribution of the diagonal elements to be fractal in the RP model allows one to adjust the phase diagram and change the location of the Anderson localization transition γ_{AT} . We have derived an analytical expression Eq. (10) that relates the Hausdorff dimension of the disorder to the fractal dimension of the eigenstates in the RP Hamiltonian, and have confirmed our findings through exact numerical computations. Furthermore, we have shown that one can manipulate the disorder

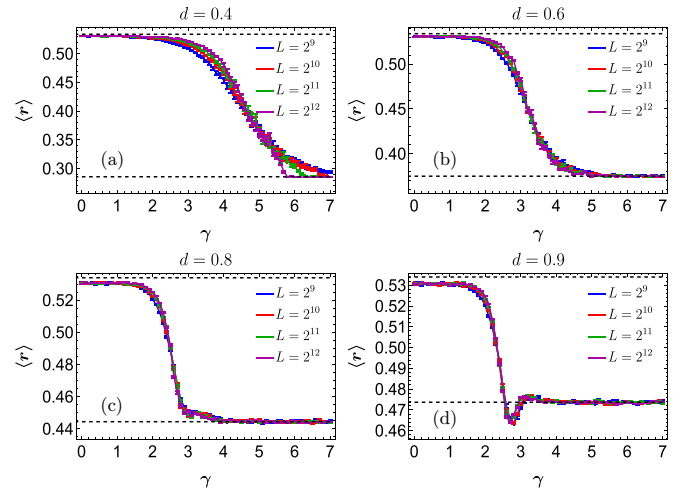


FIG. 5. $\langle r \rangle$ statistics vs γ , averaged over the entire spectrum for fractal disorder with (a) $d = 0.4$, (b) $d = 0.6$, (c) $d = 0.8$, (d) $d = 0.9$, and different system sizes L . The black dashed lines denote the expected values of $\langle r \rangle$ for GOE statistics and the localized phase [Eq. (19)].

dependence of the fractal dimension by utilizing a multifractal disorder. Finally, we have evaluated the implications of our modification on the eigenspectrum through level spacing ratio.

This work provides a step in the direction of usage of the fractal disorder for the controllable tunability of the phase diagrams of various disordered models.

In particular, this work opens the way to study whether such fractal diagonal disorder enhances the fractality of wave functions in other long-range models, such as the power-law banded models [52], Burin-Maksimov model [53–56], some Bethe-ansatz integrable ones [57–59], on the random graphs [60,61], or even in the interacting disordered models [4]. In all these cases (especially in the latter two), the fractal disorder may give a way for a nonergodic spatially extended phase of matter, intensively discussed and highly relevant for quantum algorithms [62] and machine learning [63]. The analysis of spectral statistics for $d \sim 1$ using a spectral form factor can also show interesting behavior at different timescales near γ_{AT} , which can help to identify more clearly the origin of the sudden dip in the $\langle r \rangle$ statistics and shed light on the spectral distribution in the critical (fractal) regime of ergodic-localized phase transitions and the structure of fractal minibands [42].

Acknowledgments. I.M.K. acknowledges the support by the European Research Council under the European Union’s Seventh Framework Program Synergy ERC-2018-SyG HERO-810451. M.S. acknowledges support of the projects J1-2463 of the Slovenian Research Agency and EU via QuantERA grant T-NiSQ. R.G. acknowledges support from UKRI Grant No. EP/R029075/1.

- [1] F. Evers and A. D. Mirlin, Anderson transitions, *Rev. Mod. Phys.* **80**, 1355 (2008).
 [2] D. Basko, I. Aleiner, and B. Altshuler, Metal-insulator transition in a weakly interacting many-electron system with localized single-particle states, *Ann. Phys.* **321**, 1126 (2006).

- [3] I. V. Gornyi, A. D. Mirlin, and D. G. Polyakov, Interacting Electrons in Disordered Wires: Anderson Localization and Low- T Transport, *Phys. Rev. Lett.* **95**, 206603 (2005).
 [4] D. A. Abanin, E. Altman, I. Bloch, and M. Serbyn, Colloquium: Many-body localization, thermalization,

- and entanglement, *Rev. Mod. Phys.* **91**, 021001 (2019).
- [5] J. M. Deutsch, Quantum statistical mechanics in a closed system, *Phys. Rev. A* **43**, 2046 (1991).
- [6] M. Srednicki, Chaos and quantum thermalization, *Phys. Rev. E* **50**, 888 (1994).
- [7] D. J. Luitz, N. Laflorencie, and F. Alet, Many-body localization edge in the random-field Heisenberg chain, *Phys. Rev. B* **91**, 081103(R) (2015).
- [8] N. Macé, F. Alet, and N. Laflorencie, Multifractal Scalings Across the Many-Body Localization Transition, *Phys. Rev. Lett.* **123**, 180601 (2019).
- [9] G. De Tomasi, I. M. Khaymovich, F. Pollmann, and S. Warzel, Rare thermal bubbles at the many-body localization transition from the Fock space point of view, *Phys. Rev. B* **104**, 024202 (2021).
- [10] Y. Bar Lev, G. Cohen, and D. R. Reichman, Absence of Diffusion in an Interacting System of Spinless Fermions on a One-Dimensional Disordered Lattice, *Phys. Rev. Lett.* **114**, 100601 (2015).
- [11] K. Agarwal, S. Gopalakrishnan, M. Knap, M. Müller, and E. Demler, Anomalous Diffusion and Griffiths Effects Near the Many-Body Localization Transition, *Phys. Rev. Lett.* **114**, 160401 (2015).
- [12] D. J. Luitz, N. Laflorencie, and F. Alet, Extended slow dynamical regime close to the many-body localization transition, *Phys. Rev. B* **93**, 060201(R) (2016).
- [13] D. J. Luitz and Y. Bar Lev, Anomalous Thermalization in Ergodic Systems, *Phys. Rev. Lett.* **117**, 170404 (2016).
- [14] I. Khait, S. Gazit, N. Y. Yao, and A. Auerbach, Spin transport of weakly disordered Heisenberg chain at infinite temperature, *Phys. Rev. B* **93**, 224205 (2016).
- [15] M. Žnidarič, A. Scardicchio, and V. K. Varma, Diffusive and Subdiffusive Spin Transport in the Ergodic Phase of a Many-Body Localizable System, *Phys. Rev. Lett.* **117**, 040601 (2016).
- [16] Y. Bar Lev, D. M. Kennes, C. Klöckner, D. R. Reichman, and C. Karrasch, Transport in quasiperiodic interacting systems: From superdiffusion to subdiffusion, *Europhys. Lett.* **119**, 37003 (2017).
- [17] S. Bera, G. De Tomasi, F. Weiner, and F. Evers, Density Propagator for Many-Body Localization: Finite-Size Effects, Transient Subdiffusion, and Exponential Decay, *Phys. Rev. Lett.* **118**, 196801 (2017).
- [18] K. Agarwal, E. Altman, E. Demler, S. Gopalakrishnan, D. A. Huse, and M. Knap, Rare-region effects and dynamics near the many-body localization transition, *Ann. Phys.* **529**, 1600326 (2017).
- [19] D. J. Luitz and Y. Bar Lev, The ergodic side of the many-body localization transition, *Ann. Phys.* **529**, 1600350 (2017).
- [20] T. L. M. Lezama, S. Bera, and J. H. Bardarson, Apparent slow dynamics in the ergodic phase of a driven many-body localized system without extensive conserved quantities, *Phys. Rev. B* **99**, 161106(R) (2019).
- [21] S. Roy, Y. Bar Lev, and D. J. Luitz, Anomalous thermalization and transport in disordered interacting Floquet systems, *Phys. Rev. B* **98**, 060201(R) (2018).
- [22] S. Roy, I. M. Khaymovich, A. Das, and R. Moessner, Multifractality without fine-tuning in a Floquet quasiperiodic chain, *SciPost Phys.* **4**, 025 (2018).
- [23] M. Sarkar, R. Ghosh, A. Sen, and K. Sengupta, Mobility edge and multifractality in a periodically driven Aubry-André model, *Phys. Rev. B* **103**, 184309 (2021).
- [24] M. Sarkar, R. Ghosh, A. Sen, and K. Sengupta, Signatures of multifractality in a periodically driven interacting Aubry-André model, *Phys. Rev. B* **105**, 024301 (2022).
- [25] S. Aditya, K. Sengupta, and D. Sen, Periodically driven model with quasiperiodic potential and staggered hopping amplitudes: Engineering of mobility gaps and multifractal states, *Phys. Rev. B* **107**, 035402 (2023).
- [26] X. Deng, S. Ray, S. Sinha, G. V. Shlyapnikov, and L. Santos, One-Dimensional Quasicrystals with Power-Law Hopping, *Phys. Rev. Lett.* **123**, 025301 (2019).
- [27] M. Serbyn, Z. Papić, and D. A. Abanin, Thouless energy and multifractality across the many-body localization transition, *Phys. Rev. B* **96**, 104201 (2017).
- [28] N. Rosenzweig and C. E. Porter, “Repulsion of energy levels” in complex atomic spectra, *Phys. Rev.* **120**, 1698 (1960).
- [29] V. E. Kravtsov, I. M. Khaymovich, E. Cuevas, and M. Amini, A random matrix model with localization and ergodic transitions, *New J. Phys.* **17**, 122002 (2015).
- [30] D. Facoetti, P. Vivo, and G. Biroli, From non-ergodic eigenvectors to local resolvent statistics and back: A random matrix perspective, *Europhys. Lett.* **115**, 47003 (2016).
- [31] K. Truong and A. Ossipov, Eigenvectors under a generic perturbation: Non-perturbative results from the random matrix approach, *Europhys. Lett.* **116**, 37002 (2016).
- [32] C. Monthus, Statistical properties of the Green function in finite size for Anderson localization models with multifractal eigenvectors, *J. Phys. A: Math. Theor.* **50**, 115002 (2017).
- [33] E. Bogomolny and M. Sieber, Eigenfunction distribution for the Rosenzweig-Porter model, *Phys. Rev. E* **98**, 032139 (2018).
- [34] D. Venturelli, L. F. Cugliandolo, G. Schehr, and M. Tarzia, Replica approach to the generalized Rosenzweig-Porter model, *SciPost Phys.* **14**, 110 (2023).
- [35] P. von Soosten and S. Warzel, Non-ergodic delocalization in the Rosenzweig-Porter model, *Lett. Math. Phys.* **109**, 905 (2018).
- [36] V. E. Kravtsov, I. M. Khaymovich, B. L. Altshuler, and L. B. Ioffe, Localization transition on the random regular graph as an unstable tricritical point in a log-normal Rosenzweig-Porter random matrix ensemble, [arXiv:2002.02979](https://arxiv.org/abs/2002.02979).
- [37] I. M. Khaymovich, V. E. Kravtsov, B. L. Altshuler, and L. B. Ioffe, Fragile ergodic phases in log-normal Rosenzweig-Porter model, *Phys. Rev. Res.* **2**, 043346 (2020).
- [38] G. Biroli and M. Tarzia, Lévy-Rosenzweig-Porter random matrix ensemble, *Phys. Rev. B* **103**, 104205 (2021).
- [39] I. M. Khaymovich and V. E. Kravtsov, Dynamical phases in a “multifractal” Rosenzweig-Porter model, *SciPost Phys.* **11**, 045 (2021).
- [40] A. G. Kutlin and I. M. Khaymovich, Anatomy of the eigenstates distribution: A quest for a genuine multifractality (unpublished).
- [41] G. De Tomasi and I. M. Khaymovich, Non-Hermitian Rosenzweig-Porter random-matrix ensemble: Obstruction to the fractal phase, *Phys. Rev. B* **106**, 094204 (2022).
- [42] B. Altshuler and V. Kravtsov, Random Cantor sets and minibands in local spectrum of quantum systems, *Ann. Phys.* **169300** (2023).

- [43] Unlike the non-Hermitian case, where $1 < d < 2$ does change the phase diagram [41].
- [44] See Supplemental Material at <http://link.aps.org/supplemental/10.1103/PhysRevB.108.L060203> for technical details and it includes Refs. [30,32,33,40,41].
- [45] Note that the strength of the diagonal elements is obtained from a fractal distribution, and not their spatial spread.
- [46] G. de Tomasi, M. Amini, S. Bera, I. M. Khaymovich, and V. E. Kravtsov, Survival probability in generalized Rosenzweig-Porter random matrix ensemble, *SciPost Phys.* **6**, 014 (2019).
- [47] W. Buijsman and Y. B. Lev, Circular Rosenzweig-Porter random matrix ensemble, *SciPost Phys.* **12**, 082 (2022).
- [48] O. Dovgoshey, O. Martio, V. Ryazanov, and M. Vuorinen, The Cantor function, *Expo. Math.* **24**, 1 (2006).
- [49] B. C. Arnold, *Pareto Distributions* (International Cooperative Publishing House, Fairland, MD, 1983).
- [50] V. Oganessian and D. A. Huse, Localization of interacting fermions at high temperature, *Phys. Rev. B* **75**, 155111 (2007).
- [51] Y. Y. Atas, E. Bogomolny, O. Giraud, and G. Roux, Distribution of the Ratio of Consecutive Level Spacings in Random Matrix Ensembles, *Phys. Rev. Lett.* **110**, 084101 (2013).
- [52] A. D. Mirlin, Y. V. Fyodorov, F.-M. Dittes, J. Quezada, and T. H. Seligman, Transition from localized to extended eigenstates in the ensemble of power-law random banded matrices, *Phys. Rev. E* **54**, 3221 (1996).
- [53] A. L. Burin and L. A. Maksimov, Localization and delocalization of particles in disordered lattice with tunneling amplitude with r^{-3} decay, *Pis'ma Zh. Eksp. Teor. Fiz.* **50**, 304 (1989) [*JETP Lett.* **50**, 338 (1989)].
- [54] X. Deng, V. E. Kravtsov, G. V. Shlyapnikov, and L. Santos, Duality in Power-Law Localization in Disordered One-Dimensional Systems, *Phys. Rev. Lett.* **120**, 110602 (2018).
- [55] P. A. Nosov, I. M. Khaymovich, and V. E. Kravtsov, Correlation-induced localization, *Phys. Rev. B* **99**, 104203 (2019).
- [56] X. Deng, A. L. Burin, and I. M. Khaymovich, Anisotropy-mediated reentrant localization, *SciPost Phys.* **13**, 116 (2022).
- [57] R. Richardson, A restricted class of exact eigenstates of the pairing-force Hamiltonian, *Phys. Lett.* **3**, 277 (1963).
- [58] R. Richardson and N. Sherman, Exact eigenstates of the pairing-force Hamiltonian, *Nucl. Phys.* **52**, 221 (1964).
- [59] R. Modak, S. Mukerjee, E. A. Yuzbashyan, and B. S. Shastry, Integrals of motion for one-dimensional Anderson localized systems, *New J. Phys.* **18**, 033010 (2016).
- [60] V. E. Kravtsov, B. L. Altshuler, and L. B. Ioffe, Non-ergodic delocalized phase in Anderson model on Bethe lattice and regular graph, *Ann. Phys.* **389**, 148 (2018).
- [61] K. Tikhonov and A. Mirlin, From Anderson localization on random regular graphs to many-body localization, *Ann. Phys.* **435**, 168525 (2021).
- [62] V. N. Smelyanskiy, K. Kechedzhi, S. Boixo, S. V. Isakov, H. Neven, and B. Altshuler, Nonergodic Delocalized States for Efficient Population Transfer within a Narrow Band of the Energy Landscape, *Phys. Rev. X* **10**, 011017 (2020).
- [63] K. Kechedzhi, V. N. Smelyanskiy, J. R. McClean, V. S. Denchev, M. Mohseni, S. V. Isakov, S. Boixo, B. L. Altshuler, and H. Neven, Efficient population transfer via non-ergodic extended states in quantum spin glass, [arXiv:1807.04792](https://arxiv.org/abs/1807.04792).